Causal influences in primate cerebral cortex during visual pattern discrimination

Hualou Liang,[CA] Mingzhou Ding, Richard Nakamura[1] and Steven L. Bressler

Center for Complex Systems and Brain Sciences, Florida Atlantic University, 777 Glades Road, Boca Raton, FL 33431; [1]Laboratory of Neuropsychology National Institute of Mental Health, Bethesda, MD 20892, USA

[CA]Corresponding Author

Received 24 May 2000; accepted 22 June 2000

Anatomical studies of the visual cortex demonstrate the existence of feedforward, feedback and lateral pathways among multiple cortical areas. Yet relatively little evidence has previously been available to show the causal influences of these areas on one another during visual information processing. We simultaneously recorded event-related local field potentials (LFPs) from surface-to-depth bipolar electrodes at six sites in the ventral region of the right hemisphere visual cortex in a highly trained macaque monkey during performance of a visual pattern discrimination task. Applying a new statistical measure, the short-time directed transfer function (STDTF), to the LFP data set, we charted the changing strength and direction of causal influence between these cortical sites on a fraction-of-a-second time scale. We present results showing, for the first time, the dynamics of distinct feedforward, feedback and lateral influences in the ventral portion of the primate visual cortex during visual pattern processing. *NeuroReport* 11:2875–2880 © 2000 Lippincott Williams & Wilkins.

Key words: Adaptive multivariate autoregression model (AMVAR); Bottom-up; Causal influences; Feedback; Feedforward; Local field potentials (LFP); Short-time directed transfer function (STDTF); Top-down; Visual cortex

INTRODUCTION

Interaction is ubiquitous in the nervous system, taking place at every level of organization. In the primate visual cortex, one form of interaction occurs at the level of cortical areas, which are mostly connected via reciprocal pathways. Activity is transmitted from the primary visual (striate) cortex to multiple higher level cortical areas by feedforward projection pathways, and from higher to lower visual areas by feedback projections [1,2]. Feedback pathways are thought to play a role in the attentional modulation and interpretation of visual information [3–6], and a number of theoretical formulations have been proposed to explain the inter-relationship between feedforward (bottom-up) and feedback (top-down) influences [7–11]. However, despite significant progress in tracing the anatomical pathways between visual cortical areas, understanding the role of interareal functional relations in vision has been hampered by a lack of direct neurophysiological observation of feedforward and feedback effects.

To directly monitor these effects in the visual cortex, we employed multiple microelectrode local field potential (LFP) recording at sites in striate, prestriate, and inferior temporal areas of a monkey performing a visual pattern discrimination task. The cortical event-related LFP was considered to be an appropriate signal for observing interareal relations because it reflects the spatial summation that is an important characteristic of communication between cortical areas [12,13]. The LFP offers distinct advantages that complement other measures of neural function. Specifically, it provides millisecond temporal resolution equivalent to that of single-unit recording, and greater spatial localization than that of PET and fMRI.

Our analysis of visual cortical LFPs was based on a newly developed method, called adaptive multivariate autoregressive (AMVAR) modeling [14], which provides a detailed depiction of the spatio-temporal dynamics of cortical activity. We evaluated feedforward and feedback causal influences in visual cortical LFP data with the short-time directed transfer function (STDTF), a statistical index of directional influence that is derived from the AMVAR time series model. We used the STDTF to compare the strength and timing of feedforward and feedback causal influence between visual cortical sites on a very short time scale while the monkey processed task-related visual information. In this way, we sought to assess the patterning in space and time of processing-related causal influences, and to determine whether this could reveal any principles of cortical independency underlying visual function.

MATERIALS AND METHODS

Behavioral task: Experiments were performed in the Laboratory of Neuropsychology at the National Institute of Mental Health. Animal care was in accordance with institutional guidelines. Surgical procedures have been described previously [15]. A highly trained rhesus macaque monkey performed a visuomotor pattern discrimination task in which it discriminated two different stimulus

types: diamonds or lines. The computer-generated stimulus set consisted of four diagonal patterns with two dots at opposite comers of an outer square, 6 cm per side, and two dots at opposite comers of a concentric inner square, 2 cm per side. The outer and inner dots were slanted in the same direction in two patterns (lines), and in opposite directions in the other two (diamonds). No single dot could be used to discriminate between diamond and line types.

The monkey was trained to begin each trial by depressing a lever with the preferred hand. The stimulus appeared for 100 ms at a random interval from 0.5 to 1.25 s following task initiation. Correct behavior consisted of the monkey releasing the lever in response to one stimulus pattern type (go trials) and maintaining lever depression to the other (no-go trials). On correct go trials, the monkey was provided with a water reward 500 ms after stimulus onset if the lever was released before that time. On correct no-go trials, the lever remained depressed for 500 ms poststimulus, and was released thereafter. Equiprobable go and no-go trials were randomly presented in 1000 trial sessions lasting about 45 min. The contingency of behavioral response on pattern type was reversed across sessions.

Recording: Bipolar (surface-to-depth) local event-related LFPs were recorded simultaneously from 15 chronically implanted electrodes at striate, prestriate and inferior temporal, parietal, motor and frontal sites in the cerebral hemisphere. LFP time series data were sampled at 200 points/s from around 115 ms prior to stimulus onset to 500 ms after stimulus onset in each trial of a session, and stored as 12-bit numbers. Trials from sessions having mixed response contingencies were pooled to form data sets for each stimulus type (diamond or line) in which the numbers of go and no-go trials were balanced.

Data analysis: During cognitive processing, the state of the brain undergoes rapid change from anticipation to perception to action, giving rise to a nonstationary LFP time series. Suppose that $X_t = (x_{1t}, x_{2t}..., x_{pt})^T$ are data from p LFP channels at time t. It has been shown [14] that within a short time window of 50 ms or so the LFP is approximately stationary and can be well represented by the multivariate autoregressive (MVAR) model:

$$\sum_{k=0}^{m} A_k X_{t-k} = E_t$$

where E_t is a temporally uncorrelated residual error vector, and A_k are $p \times p$ coefficient matrices which are obtained by solving the multivariate Yule-Walker equation (of size mp^2) using the Levinson, Wiggins and Robinson (LWR) algorithm [16]. The model order m is determined by the Akaike information criterion (AIC) [17]. Data from multiple trials are treated as realizations of the same underlying stochastic process and are combined to produce the estimation of the model coefficients.

The basis for evaluating the direction of influences between channels is the concept of Granger causality [18]. For two simultaneously measured time series, one series is called causal to the second if the residual error for the second series at the present time is reduced by including the past measurements from the first series in the regression model. We used the method of Kaminski and Blinowska [17]. Let H(f) denote the transfer function given by:

$$H(f) = \left(\sum_{j=0}^{m} A(j) e^{-2\pi i j f} \right)^{-1}$$

The directed transfer function is defined as the magnitude (or the squared magnitude) of the matrix element $H_{ji}(f)$ which measures the causal influence from site i to j. Recent work has shown that the DTF function is equivalent to a spectral measure of Granger causality [19], thus allowing us to take advantage of the full multivariate power and convenience of the DTF function while preserving the well-accepted interpretation of Granger causality. We note that our implementation of the DTF is different from the original measure developed by Kaminski and Blinowska [17] in that we do not normalize these transfer function values.

Short-time directed transfer function (STDTF) analysis is based on the AMVAR (adaptive MVAR) approach involving the adaptive estimation of the MVAR model coefficients with a sliding analysis window [14]. A 50-ms-long (10 points) analysis window was stepped point by point through the entire duration of the trial. In each window, data from all 888 trials and 15 sites were used to estimate the MVAR model and compute DTF spectra from it. The result was a time-frequency plot of the STDTF in both directions for all pairs of sites. In addition, a bootstrap resampling procedure was employed in which the STDTF was computed for 100 resamples of the 888 trials. This procedure, yielding a resample mean and variance of the STDTF at each time, was used for statistical significance assessment (see below).

In this study, we restricted our analysis of causal influences to the recording sites in the ventral region of the visual cortex: three sites in the striate cortex, two in prestriate cortex, and one in the inferior temporal cortex (Fig. 1). Feedforward influences were from striate to prestriate and inferior temporal, and from prestriate to inferior temporal. Feedback influences were from inferior temporal to prestriate and striate, and from prestriate to striate. Lateral influences were between striate or between

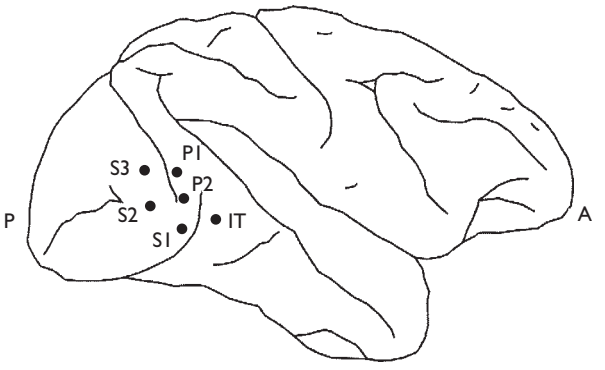

Fig. 1. Right hemisphere of rhesus macaque monkey GE, showing the locations of recording sites in striate (3), prestriate (2) and inferior temporal (1) cortex. At each site, the field potential was localized by differential transcortical recording from a pair of microelectrodes.

prestriate sites. It is important to emphasize that the DTF function is purely statistical in nature and is neutral with respect to the anatomical pathway(s) by which influences are exerted.

For each direction of each site pair, we first located the maximum peak of poststimulus STDTF in both frequency and time. We then determined whether this peak was significantly above the STDTF level in a baseline period which extended from 60 ms prior to, until 15 ms following stimulus onset. Significant peaks were those which the bootstrap mean peak value was greater than the baseline mean by a one-tailed t comparison ($p < 0.02$), following correction for multiple t-tests by Dunn's method.

For those directions and pairs having significant peaks, we next determined the onset and offset times of the stimulus-related STDTF response. Considering the STDTF time course at the peak frequency, as well as surrounding frequencies for which the STDTF exceeded the half-maximum peak amplitude, we determined the earliest significant poststimulus STDTF change at each of these frequencies. This significant change was computed in relation to a threshold level set at 2 s.d. above the mean STDTF of the baseline period. The onset time was taken as the first time point out of at least three consecutive time points following the baseline period that exceeded the baseline level. The offset time was the time at which the STDTF fell below the baseline threshold.

RESULTS

The strength and direction of short-time causal influences were first examined in time-frequency STDTF plots during stimulus processing for all site pairs in the ventral region of the primate visual cortex. Significant stimulus-related increases in STDTF were observed in the spectral vicinity of 12 Hz, with peaks generally occurring in the time period from 50 ms to 160 ms after stimulus onset (Fig. 2). These poststimulus episodes of elevated STDTF showed feedforward (Fig. 2a), feedback (Fig. 2b) and lateral effects. The coherence analysis showed similar result [14,20–22] (Fig. 2c), but it should be emphasized that the STDTF provides additional information on directional influence.

All site pairs showed significant causal influence in both directions, based on poststimulus STDTF peaks that were significantly above the baseline level at $p < 0.05$ (Table 1). Different pairs and directions, however, varied widely in the degree to which they were significant. In order to illustrate the spatial patterning of feedforward, feedback, and lateral causal influence, we present in Fig. 3 diagrams showing the most significant ($p < 10^{-6}$) poststimulus STDTFs for the diamond (Fig. 3a) and line (Fig. 3b) stimulus types. The sites are represented in these diagrams as nodes, and the most significant STDTFs as lines connecting the nodes, with arrowheads indicating the direction of influence. We emphasize that these arrows represent statistical causal influences, and not necessarily transmission

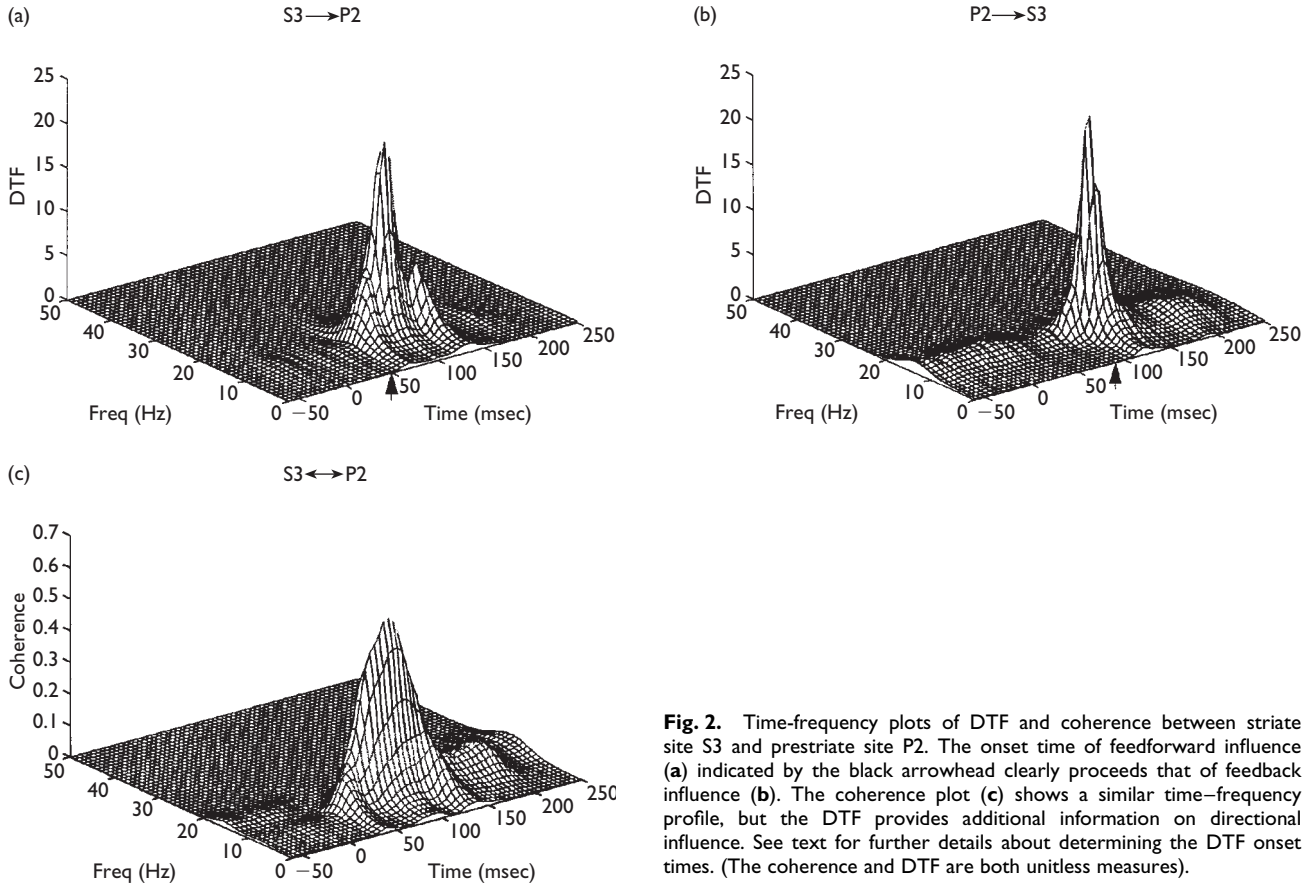

Fig. 2. Time-frequency plots of DTF and coherence between striate site S3 and prestriate site P2. The onset time of feedforward influence (**a**) indicated by the black arrowhead clearly proceeds that of feedback influence (**b**). The coherence plot (**c**) shows a similar time–frequency profile, but the DTF provides additional information on directional influence. See text for further details about determining the DTF onset times. (The coherence and DTF are both unitless measures).

Table 1. Significance and dominant frequencies of feedforward (FF), feedback (FB), and lateral causal influences for stimulus types of line and diamond.

		Diamond		Line	
Direction	Connection	Frequency (Hz)	*p*-value	Frequency (Hz)	*p*-value
FF	S1→P1	11	2×10^{-3}*	10	1×10^{-5}**
	S2→P1	12	8×10^{-6}**	12	2×10^{-7}***
	S3→P1	13	5×10^{-6}**	13	2×10^{-8}***
	S1→P2	9	4×10^{-8}***	10	2×10^{-7}***
	S2→P2	13	3×10^{-11}***	13	9×10^{-11}***
	S3→P2	13	1×10^{-16}***	12	3×10^{-16}***
	S1→IT	9	2×10^{-5}**	9	3×10^{-6}**
	S2→IT	9	6×10^{-10}***	9	1×10^{-11}***
	S3→IT	13	1×10^{-9}***	13	3×10^{-6}**
	P1→IT	10	3×10^{-5}**	10	1×10^{-5}**
	P2→IT	10	2×10^{-12}***	9	1×10^{-9}***
FB	P1→S1	9	2×10^{-7}***	9	1×10^{-11}***
	P1→S2	10	3×10^{-4}*	13	9×10^{-3}*
	P1→S3	9	2×10^{-2}*	9	3×10^{-6}**
	P2→S1	12	2×10^{-16}***	12	6×10^{-9}***
	P2→S2	13	2×10^{-14}***	12	2×10^{-9}***
	P2→S3	10	7×10^{-11}***	9	2×10^{-11}***
	IT→S1	11	4×10^{-7}***	13	8×10^{-9}***
	IT→S2	11	1×10^{-5}**	13	7×10^{-10}***
	IT→S3	13	4×10^{-5}**	10	2×10^{-6}**
	IT→P1	10	4×10^{-5}**	10	4×10^{-6}**
	IT→P2	10	2×10^{-5}**	9	3×10^{-6}**
Lateral	S1→P2	9	8×10^{-7}***	10	1×10^{-4}*
	S1→S3	9	4×10^{-8}***	10	1×10^{-4}*
	S2→S3	12	5×10^{-6}**	11	2×10^{-7}***
	S2→S1	12	7×10^{-9}***	13	2×10^{-12}***
	S3→S1	13	1×10^{-10}***	13	2×10^{-10}***
	S3→S2	9	7×10^{-12}***	13	1×10^{-5}**
	P1→P2	9	1×10^{-2}*	9	7×10^{-6}**
	P2→P1	10	4×10^{-8}***	12	1×10^{-10}***

*** $p<10^{-6}$; ** $p<10^{-4}$; * $p<0.05$.

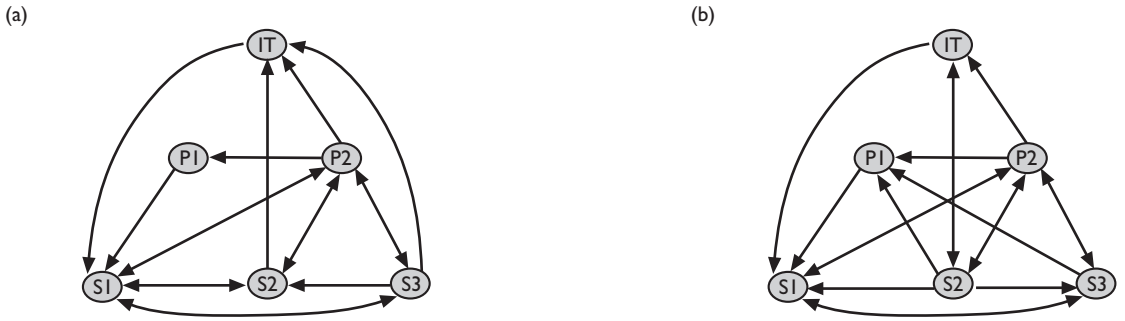

Fig. 3. Schematic diagrams illustrating causal influences among cortical sites shown in Fig. 1 for the stimulus pattern of diamond (**a**) and of line (**b**). The upward and downward arrowheads represent feedforward and feedback influences, respectively. The lines denote the existence of significant peaks ($p<10^{-6}$).

over direct axonal pathways from one site to another. The diagrams reveal that highly significant (strong) feedforward, feedback, and lateral effects occurred during visual stimulus processing.

A number of features of causal influence are evident from examination of Fig. 3 and Table 1. For both stimulus types, strong feedforward influences occur from striate to prestriate and inferior temporal, and from prestriate to inferior temporal, sites. These feedforward influences emanate from all three striate sites. There is strong convergence onto prestriate site P2 for both stimulus types, but onto site P1 only for the line type. Feedforward influences on IT come only from striate sites S2 and S3 and prestriate site P2. Strong feedback effects are seen from prestriate site P2 back to all striate sites, but from P1 only back to striate site S1. In fact, the only strong influence emanating from P1 is to S1. Although site IT receives strong feedforward influences from striate sites S2 and S3, and also from prestriate

site P2, it feeds back strong influences only to S1 (and S2 in the line condition). Lateral effects are seen among all sites in the striate cortex, but only from P2 to P1 in the prestriate cortex. These diagrams present examples of strong reciprocal influence between striate sites, between striate and prestriate sites, and, between striate and inferior temporal sites. Excluding the striate sites, the only strong influences are seen emanating from prestriate site P2.

In addition to the strength, direction, and spatial patterning of causal influence, we also investigated its onset, peak and offset timing. Figure 4 illustrates the timing differences between the feedforward (solid) and feedback (dashed) STDTF of sites S3 and P2 at 12 Hz. Vertical lines mark the onset times of these influences. The feedforward influence, from striate to prestriate, begins and peaks earlier than the feedback influence in the opposite direction. Table 2 presents the mean and standard deviation of onset, peak, and offset times of significant causal influence over all the pairs in feedforward (FF) and feedback (FB) directions for line and diamond stimulus types. A three-way ANOVA (time $\times$ direction $\times$ stimulus type) was performed on this data set. Significant main effects were found for time ($F(2,66) = 211.33$, $p < 0.0001$) and direction ($F(1,66) = 27.33$, $p < 0.0001$), but not for stimulus type. No interactions were significant. Using the Scheffé *post-hoc* test, both onset time and offset time were found to occur significantly ($p < 0.01$) earlier in feedforward than feedback directions.

DISCUSSION

Various forms of causal measures, all based on autoregressive modeling, have been applied in neurobiology since the early 1980s. Saito and Harashima [23] introduced the method of directed coherence to study the relation between a pair of data channels described by a bivariate autoregressive process. Schnider *et al*. [24] used results given by Gevers and Anderson [25] to detect feedback interactions between Parkinsonian tremor and cell activities in the thalamus. More recently, Bernasconi and König [26] applied a spectral measure developed by Geweke [27] to detect causal influences among different visual areas in the cat. All of these studies used relatively long segments of recorded data to estimate the autoregressive time series model. Hence, they were only able to detect causal effects that were averaged over these long time periods. The STDTF measure, combining the DTF function and the short window AMVAR approach, enabled us to examine cortical dynamics on a much finer time scale. The ability is critical in determining the causal influence among different cortical areas during cognitive processing.

In the time period from roughly 50 to 160 ms following the onset of the visual stimulus in a visual pattern

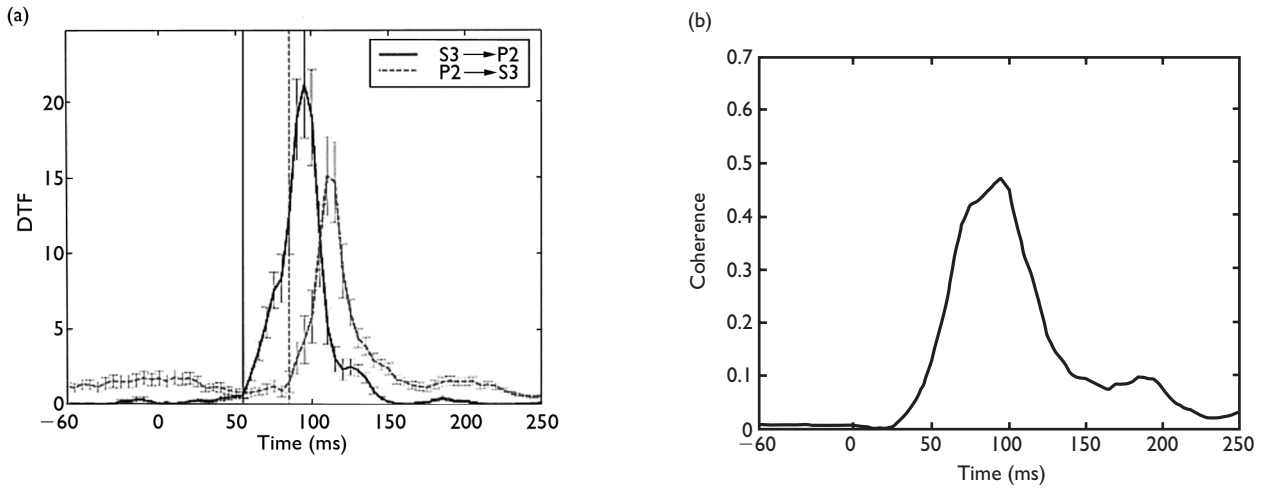

Fig. 4. Feedforward, feedback DTF time series (**a**) at a frequency of 12 Hz with error bars obtained by bootstrap resampling. The feedforward influence (solid line) from striate site S3 to prestriate site P2 occurs earlier than the feedback influence (dashed line) in the opposite direction. The vertical lines indicate the onset times of these influences. The coherence time series at 12 Hz is also shown (**b**) for comparison. The stimulus duration of 100 ms is marked by the dark horizontal bar.

Table 2. Means and standard deviations of onset, peak and offset times in ms for diamond and line in the feedforward (FF) and feedback (FB) directions

	Diamond			Line		
	Onset	Peak	Offset	Onset	Peak	Offset
FF	59 ± 8.6	95 ± 1.7	146 ± 10.2	58 ± 12.1	102 ± 12.8	146 ± 8.6
FB	74 ± 9.3	116 ± 5.6	164 ± 18.0	76 ± 12.1	119 ± 12.9	159 ± 17.7

discrimination task, we found significant increases in feedforward causal influence from sites in the striate cortex to sites in prestriate cortex and inferior temporal cortex. In addition, significant feedback influences were observed. The fact that feedback onset and offset times were significantly delayed compared with feedforward times indicates that feedback influences largely occur in response to feedforward effects. There were exceptions, however. In some cases, the feedback influence for a pair of sites began earlier than the feedforward. In other cases, a strong feedback influence was absent, even though a strong feedforward influence was observed. Thus it appears that feedback effects from a higher to a lower level in the hierarchy of the visual cortex do not always occur in direct response to feedforward influences from the lower level.

In the spatial patterning of strong causal influence, we observed convergence and divergence for both feedforward and feedback influences. We also observed strong reciprocal influences (i.e. both feedforward and feedback between two sites). These patterns are all consistent with the known anatomical connectivity of the visual cortex [2,7,28]. The observation of strong causal influences among multiple cortical areas during stimulus processing has a number of potential functional implications. First, the observed feedback influences may reflect the attentional modulation of neuronal activity in striate cortex from prestriate and inferior sources [3–6]. Second, these feedback influences may be a sign of the resolution of discrepancy between visual input and stored or expected visual patterns [9,11]. Third, evidence of divergent prestriate-to-striate feedback (Fig. 3) may promote the binding of neural activity between the recipient striate sites [7]. Finally, reciprocal feedforward and feedback effects between a pair of sites may be the manifestation of reentrant interactions postulated to be an essential component of functional integration in the cortex [29].

Comparison of the overall duration of STDTF feedforward influences between visual cortical areas was useful for addressing the question of whether those areas process information in parallel or in a serial fashion. The observed extent of feedforward influence from striate sites to prestriate sites (40–170 ms) exhibited considerable overlap with that from prestriate sites to site IT (60–190 ms). Furthermore, the feedback influences (60–200 ms from prestriate to striate and 75–165 ms from IT to prestriate) were highly overlapped in time with the feedforward influences. Taken together, our results suggest that information processing in the hierarchy of visual cortical areas is not strictly sequential, but occurs concurrently across multiple hierarchically successive visual areas [30] and involves the reciprocal interplay of feedforward and feedback influences.

CONCLUSION

The STDTF is a powerful tool for investigating dynamic causal influences in the multi-area hierarchy of the visual cortex. With this method, we measured that strength and direction of casual influences between sites in the same and different cortical areas on a very short time scale. Our results clearly show strong feedforward, feedback and lateral influences between areas in the ventral region of the primate visual cortex. We also found that feedback influences arise significantly later than feedforward influences. This suggested that feedback is largely a response to feedforward input, although exceptions to this principle indicate that feedback influences are not obligatory, and may in fact occur independently of feedforward influences. Finally, the finding that feedforward and feedback influences were concurrent for tens of milliseconds suggests that areas could engage in reciprocal interactions during this period.

REFERENCES

1. Rockland KS and Pandya, DK. *Brain Res* **179**, 3–20 (1979).
2. Felleman D and Van Essen D. *Cereb Cort* **1**, 1–47 (1991).
3. Motter BC. *J Neurophysiol* **70**, 909–919 (1993).
4. Lamme VAF, Zipser K and Spekreijse H. *Proc Natl Acad Sci USA* **95**, 3263–3268 (1998).
5. Hillyard SA and Anllo-Vento L. *Proc Natl Acad Sci USA* **95**, 781–787 (1998).
6. Zipser K, Lamme VAF and Schiller PH. *J Neurosci* **16**, 7376–7389 (1996).
7. Zeki S. *A Vision of the Brain.* Oxford: Blackwell Scientific Publications; 1993.
8. Kawato M, Hayakawa H and Inui T. *Network* **4**, 415–422 (1993).
9. Mumford D. Neuronal architectures for pattern-theoretic problems. In: Koch C and Davis JL, eds. *Large-Scale Neuronal Theories of the Brain.* Cambridge: MIT Press; 1994.
10. Ullman S. *Cerebr Cort* **5**, 1–11 (1995).
11. Grossberg S. *Spatial Vis* **12**, 163–185 (1999).
12. Bressler SL. *Brain Res Rev* **20**, 288–304 (1995).
13. Bressler SL. *Behav Brain Res* **76**, 37–49 91996).
14. Ding M, Bressler SL, Yang W *et al. Biol Cybern* **83**, 35–45 (2000).
15. Bressler SL, Nakamura R. Inter-area synchronization in macaque neocortex during a visual patterns discrimination task. In: Eeckman F and Bower J, eds. *Computation and Neural Systems.* Norwell, MA: Kluwer; 1993, pp. 515–522.
16. Morf M, Vieira A, Lee D *et al. IEEE Trans Geosci Electron* **16**, 85–94 (1978).
17. Kaminski MJ and Blinowska KJ. *Biol Cybern* **65**, 203–210 (1991).
18. Granger CWJ. *Econometrica* **37**, 424–438 (1969).
19. Kaminski MJ, Ding M and Bressler SL. *Dynam Neurosci Abstr* **47** (1999).
20. Bressler SL, Coppola R and Nakamura R. *Nature* **366**, 153–156 (1993).
21. Bressler SL, Ding M and Yang W. *Neurocomp* **26**, 625–631 (1999).
22. Liang H, Ding M and Bressler SL. *Neurocomp* **32–33**, 891–896 (2000).
23. Saito Y and Harashima H. Tracking of information within multichannel EEG record. In: Yamaguchi N and Fujisawa K, eds. *Recent Advances in EEG and EMG Data Processing.* Amsterdam: Elsevier; 1981.
24. Schnider SM, Kwong RH, Lenz FA *et al. Biol Cybern* **60**, 203–212 (1989).
25. Gevers MR and Anderson BDO. *Int J Control* **33**, 777–809 (1981).
26. Bernasconi C and König P. *Biol Cybern* **81**, 199–210 (1999).
27. Geweke J. *J Am Stat Assoc* **77**, 304–313 (1982).
28. Gilbert CD. *Cerebr Cort* **3**, 373–386 (1993).
29. Tononi G, Sporns O and Edelman GM. *Cerebr Cort* **2**, 310–335 (1992).
30. Bullier J and Nowak LG. *Curr Opin Neurobiol* **5**, 497–503 (1995).

Acknowledgements: Supported by grant IBN-9723240 from the National Science Foundation, grant MH-58190-02 from the National Institute of Mental Health, and grant N00014-99-1-0062 from US Office of Naval Research.